Presented at the Fifth International
Conference on Atomic Physics,
Berkeley, CA, July 26 - 30, 1976

LBL-5711
c.1

HYPERFINE STRUCTURE OF STORED IONS... RESULTS FOR 2s $^3He^+$

Michael H. Prior and Edmond C. Wang

August 1976

Prepared for the U. S. Energy Research and
Development Administration under Contract W-7405-ENG-48

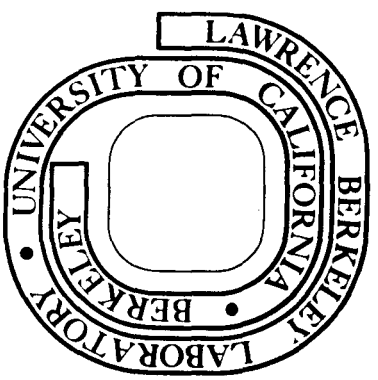

LBL-5711
c.1

DISCLAIMER

HYPERFINE STRUCTURE OF STORED IONS... RESULTS FOR 2s $^3He^+$ *

Michael H. Prior and Edmond C. Wang

Department of Physics and Lawrence Berkeley Laboratory
University of California
Berkeley, California 94720

INTRODUCTION

The study of ions and their interactions by means of storage devices which hold them for long periods encompasses a broad range of experimental effort. In the area of collision studies, treated by G. Dunn[1] at the 1974 International Conference on Atomic Physics (ICAP), it includes electron-ion recombination, spin and charge exchange, photo-dissociation, and ion-molecule reactions among others. Another broad area, the original emphasis of the technique, is the radio-frequency spectroscopy of stored ions. This area was pioneered by H. Dehmelt and his collaborators and was reported on at the first ICAP in 1968[2]. The range of possible experiments here includes the traditional domain of rf spectroscopy of atomic and molecular species; e.g. magnetic moments, hyperfine structure and fine structure. New possibilities include the use of lasers as optical pumping sources and, beyond the rf frequency range, one expects two-photon laser spectroscopy on stored ions to emerge[3]. Closely allied to the above, but distinguished by their uniqueness and high degree of refinement, are the experiments of the U. Washington group to measure the anomalous magnetic moment of a single electron[4].

A less explored but potentially large area for study is the measurement of the lifetimes of metastable excited ionic states[3,5].

Of course, one must note the very large effort currently underway world wide to understand and manipulate the behavior of high density plasmas in any of the many controlled thermonuclear reactor (CTR) experiments. The CTR devices differ markedly from the ion

traps under discussion here; there is, however, some overlap in the sense that some of the processes of interest[6] to the CTR program for diagnostic and other reasons (e.g., charge exchange, recombination and decay rates of long-lived excited ionic states) are amenable to study with small scale ion traps.

This report lies in the area of radio-frequency spectroscopy and describes the measurement by Dr. E.C. Wang and the author, of the hyperfine structure (hfs) of the metastable 2s state of the $^3He^+$ ion. A brief report of our early results has appeared previously[7].

HFS MEASUREMENTS ON STORED IONS

By way of placing our work in perspective, a brief discussion of the advantages and drawbacks of the ion-storage technique as applied to the study of the hfs of ions, as well as a summary of previous ion-storage hfs measurements follows. For detailed discussion of many of the topics, the reader is referred to the reviews by Dehmelt[8].

One of the strong points of ion-storage methods for the study of hfs is the long observation times available to induce a hyperfine transition. Ions have been stored without loss for periods of many hours (see e.g., Ref. 1) so that, in principle, resonance line widths of unprecedented narrowness (say $\approx 10^{-4}$ Hz) might be imagined for experiments on ionic ground states. The real questions of the feasibility and utility of an experiment with such a narrow line (requiring perhaps several days to sweep over) detract from its obvious appeal as a tour-de-force. In fact, other considerations often limit the line width and precision of a measurement to less than that allowed on the basis of the ion storage time alone. The quadratic Doppler effect caused by the ion velocity distribution (finite ion temperature) is an example. None-the-less valuable measurements have been made on lines whose widths are only a few Hz[9,10]; this is far narrower than typical atomic beam magnetic resonances linewidths (generally > 1 kHz).

The fact that stored ions are unperturbed by collision with background gas atoms is, of course, responsible for their long storage times and is achieved by the use of standard ultra high vacuum techniques to reduce the background pressure. Ion-ion collisions take place typically at rates of .1 to 10^3 sec^{-1} depending on ion density and temperature, but, because of the long range coulomb force, the wave function overlap is very small and usually results in no significant perturbation to the internal properties of the ions.

Finally, one might include as an advantage of the ion storage

technique, the non-destructive detection of the number of stored ions by resonant excitation of their motion. Scattering of resonant optical photons[3,10] is also a useful non-destructive probe of the number of stored ions and can serve to monitor Zeeman sublevels as well.

On the negative side, the number of stored ions is not large being typically 10^6 to 10^8 for ground state ions and perhaps 10 to 1000 times less for excited ionic states (e.g. 2s $^3He^+$). Thus the signal to noise ratio of resonances is low and may typically require an hour of integration to achieve a value of 10/1. Monitoring of substate populations via scattering of resonant optical photons may well improve this situation for favorable cases in the near future.

A further weakness is the fact that to date no generally applicable technique for hyperfine state selection exists. Each ion requires its own special solution and one does not have a counterpart for ions of the atomic beam magnetic resonance method which has had such wide application to virtually any paramagnetic atom or molecule. Tunable lasers may somewhat rescue this state of affairs by allowing the technique of optical pumping to assume this role, at least for a subset of favorable ions.

Finally, the radio frequency spectrum may well be perturbed by the confining fields and the ion motion (e.g. Stark, Zeeman and Doppler effects). This is usually not a serious problem as one has considerable flexibility in selection of the type of fields and control of their magnitude. Corrections can be made with some confidence; and, if necessary, extrapolation can be made to field free values.

In the past 14 years or so, since the pioneering work of H. Dehmelt and co-workers[11], two types of ion trap have been used extensively and their properties are well described in Dehmelt's reviews[8]. These are the static field Penning trap and the dynamic field Paul or rf quadrupole trap. Both use a cylindrically symmetric electric potential of the form

$$\Phi(r,z) = U \cdot \frac{2z^2 - r^2}{2z_o^2 + r_o^2}$$

whose equipotentials are the familiar hyperbolas of revolution. U is the potential applied between the cap electrodes separated by $2z_o$ and the ring electrode whose inside radius is r_o; typically z_o, r_o are a few centimeters or less. In the case of the Penning trap (PT), U is constant, usually in the range of 1 to 100 volts,

and; in addition, there is present a vector potential $\bar{A} = \bar{r} \times \hat{z} H$ producing a constant magnetic field of magnitude H ($\simeq$ 100 to 10,000 gauss) along the z-axis. Ion motion consists of simultaneous harmonic oscillation parallel to the z-axis, cyclotron motion about the magnetic field lines and a magnetron or $\bar{E} \times \bar{H}$ drift of the cyclotron orbit center about the trap axis.

The rf quadrupole trap (RFQT) uses an oscillating electric potential, i.e., $U = U_o \cos\Omega t$, with Ω typically $\simeq .1 \rightarrow 1.5$ MHz, and $U_o \simeq 100$ to 1000 V and no magnetic field. Ion motion is determined by solution of Mathieu equations and consists of a small amplitude high frequency oscillation at or near Ω and lower frequency larger amplitude harmonic motion in an effective potential ψ of the form

$$\psi = \frac{1}{2}k\cdot(\langle r\rangle^2 + 4\langle z\rangle^2),$$

where $\langle r\rangle$ and $\langle z\rangle$ are r and z coordinates averaged over the high frequency motion.

This brief description of the RFQT and PT schemes will allow some comparison with the purely electrostatic trap design we have used in our experiment. The electrostatic trap was first described by K.H. Kingdon[12] in 1923. More recently, R.G. Herb[13] and associates have developed this configuration as an ionization gauge and, as such, it is known as an "Orbitron." The device consists of a negatively charged wire inside a closed, coaxial cylinder; it has not been applied to the rf spectroscopy of ions previously and it will be discussed in somewhat more detail in a following section.

A summary of published ion-storage hfs measurements is presented in Table I. The entrees are arranged chronologically and the definition of ion-storage is broadened somewhat to include the ion-beam experiment of Novick and Commins[14] on 2s $^3He^+$. (The drifting ions in the beam can be regarded as inertially "confined" during their transit time through the apparatus). This is done because, for many years their experiment stood as the only precise measurement of hfs in a free ion and it forms the point of departure for the work we have done recently on 2s $^3He^+$.

Things to note from Table I are the large values of $Q = \nu/\Gamma$, the ratio of resonance frequency to line width, achieved and the different state selection and analysis schemes used. One notes that all the work except that on 2s $^3He^+$ has been carried out with rf quadrupole traps.

Table I. Hfs Measurements on Stored Ions

Ion	State	hfs freq. (MHz)	Q	Type of Trap	State Selection/ Analysis	Authors(Year)
$^3He^+$	2s	1083.3···	1.0×10^4	ion-beam	resonant μwave quenching	Novick, Commins[a](58)
H_2^+	K=1,2; v=4→8	3.9··· →1248.5···	2.4×10^6	RFQT	polarized photo-dissociation	Jefferts[b](68,69)
$^3He^+$	1s	8665.6···	9.0×10^8	RFQT	spin exchange/ spin dependent charge exchange	Scheussler, Fortson, Dehmelt[c](69)
$^{199}Hg^+$	g.s. $^2S_{1/2}$	40507.4···	5.0×10^9	RFQT	optical pumping/ resonant fluores-cence	Major, Werth[d](73)
$^3He^+$	2s	1083.3···	1.0×10^6	electro-static	resonant μwave quenching	Prior, Wang[e](75,76)

[a]Ref 14; [b]Ref 15; [c]Ref. 9; [d]Ref. 10; [e]Ref. 7 and this report.

A motivation for the work summarized in Table I has been (H_2^+ and $^3He^+$) to make precision measurements in simple systems where good tests of theory seem possible. In addition, for H_2^+ there was motivation to determine the hfs spectrum of this simplest molecule for astrophysical reasons. For the heavy ion $^{199}Hg^+$, Major and Werth[10] accomplished the first optical pumping of stored ions and the motivation here was, in large measure, the desire to make progress toward the realization of a new time standard. This goal has been often discussed (see e.g., Ref. 16) as a possibility for stored-ion rf spectroscopy, but has yet to be achieved. The low signal to noise ratio of the resonances is the major impediment.

RATIONALE FOR AN IMPROVED 2s $^3He^+$ HFS VALUE

One of the most precisely known quantities in atomic physics is the ground state hfs, $\Delta\nu_1$, in the hydrogen atom. With a fractional uncertainty of $\pm 1.4 \times 10^{-12}$, the experimental value[17] stands as a strong challenge to theory in the one-electron atom. Unfortunately, theory[18] is blocked by uncertainty in the nuclear size and polarizability contributions (-34.6±5.0 ppm) to the nuclear correction $\delta_1(H)$. Thus there are many interesting QED corrections to simple theory which are of the same size or smaller than the uncertainty in $\delta_1(H)$ which cannot be tested by direct comparison with the experimental value. The motivation to extend theory at this level or beyond is thus small.

It is possible to sharply reduce the importance of nuclear corrections, if one has available an additional precision hfs measurement in an excited state. For practical reasons this is restricted to $\Delta\nu_2$, the metastable 2s state hfs. One forms the difference, $D_{21} \equiv 8\Delta\nu_2 - \Delta\nu_1$, which is much less sensitive to nuclear structure (whose leading terms scale like n^{-3}) than $\Delta\nu_1$ or $\Delta\nu_2$ separately. The situation is improved for the QED terms as well. The coefficient of the $(\alpha/\pi)(Z\alpha)^2$ correction term is known exactly for D_{21} (it is -5.5515)[19,20], whereas in the expression for $\Delta\nu_1$ it has an estimated uncertainty of 27% (18.36±5)[21]. It is evidently easier to calculate the QED term differences which contribute to D_{21}, thanks to cancellation of the more difficult state independent terms.

The situation in $^3He^+$ is analogous to that in H except that the nuclear size correction is considerably larger and is less precisely known; two estimates have been made by Sessler & Foley[22] which yielded -183 ppm and -146 ppm depending on the nuclear wave functions used.

The experimental value of D_{21} for $^3He^+$ prior to our work was 1.1901(16) MHz (based on Refs. 9 and 14) with the uncertainty due almost exclusively to that in the $\Delta\nu_2$ measurement of Novick and

Commins. This is to be compared with a theoretical value of 1.1898(5) MHz where the uncertainty is an estimate of uncalculated terms. The size of these terms could be revealed by a more precise value of $\Delta\nu_2$, and this was the motivation for our work.

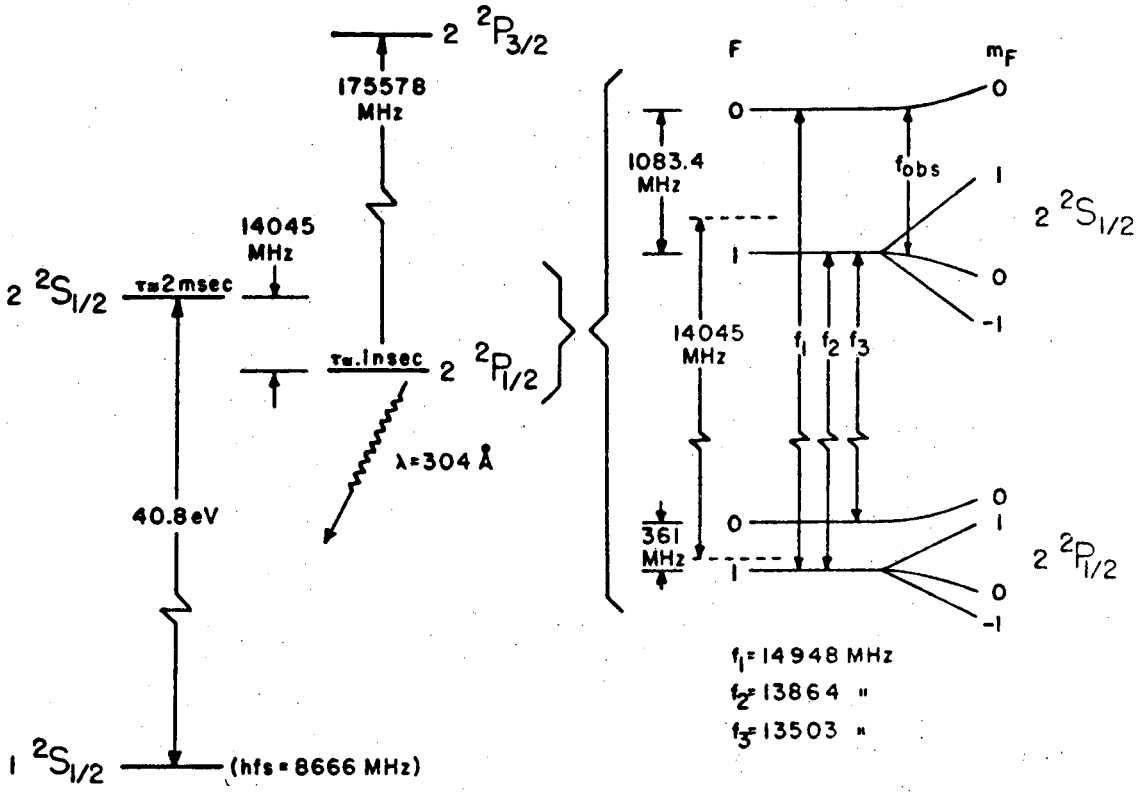

Fig. 1 Energy levels in $^3He^+$.

METHOD OF MEASUREMENT

Fig. 1 shows the energy level structure of $^3He^+$ in the n = 1 and 2 states. Our method consists of creating 2s ions inside an ion-storage device (ion trap) by electron impact on ^3He gas at low pressure (about 4.0×10^{-6} torr). While the ions are confined, we preferentially remove those in either the F = 0 or F = 1 hyperfine states by application of a microwave power pulse tuned near the hyperfine split Lamb shift transitions f_1 or f_2, f_3. (The 1600MHz width of the $2^2P_{\frac{1}{2}}$ states compared to their 360 MHz ^{3}hfs splitting causes the f_2 and f_3 resonances to be unresolved.) Once in one of the $2^2P_{\frac{1}{2}}$ states, an ion decays with a lifetime of 10^{-10} sec to the 1s ground state by emitting a 304 Å photon. Population of the depleted 2s hyperfine level can be restored by transfer from the

undepleted level by means of the $\Delta F = 1$, $\Delta m_F = 0$ hyperfine transition marked f_{obs} in Fig. 1. This is done after the microwave state selection by a suitably polarized oscillating magnetic field pulse set near the hfs frequency. A second microwave pulse is then applied and photon detectors and associated electronics count the number of ensuing 304 Å photons. Counts collected versus frequency applied during the middle hfs transition period yield a resonance curve, ideally at the unperturbed hfs frequency, $\Delta\nu_2$. This is the same state-selection and resonance detection scheme used in the experiment of Novick & Commins[14], the difference being the use of ion-storage rather than an ion-beam; this requires time-like rather than spatial separation of functions. By storing the ions we achieve longer measurement times and have achieved line widths less than 1kHz (FWHM) compared to 100kHz in the work of Novick and Commins. The precision of a resonance line center determination can be roughly estimated as the line width divided by the signal-to-noise ratio. Our signal-to-noise ratio is not as good as that achieved in the beam experiment so we do not gain the full factor of 100 or so indicated by the reduction in line width; in fact, we have achieved about a factor of 20 improvement.

THE ELECTROSTATIC ION TRAP

It was our intention to obtain an experimental configuration which would produce resonances at essentially the field free hyperfine frequency in order to avoid the need for large corrections and extrapolations. For this reason, we did not choose to use a Penning type ion trap such as that used previously to measure the 2s lifetime in $^4He^+$ (Ref 5). The magnetic field needed to operate the trap would have required a large Zeeman effect correction. The large amplitude electric fields associated with radio-frequency quadrupole ion traps were considered prohibitive because of the associated Stark quenching of the 2s state. For these reasons we adopted a purely electrostatic confinement scheme. Fig. 2 shows a cross section view of our device. It is a closed cylinder with a central rod maintained at a negative potential with respect to the grounded walls. $^3He^+$ ions are created by impact with electrons emitted from a filament located outside the bottom end of the cylinder. The electrons move roughly parallel to the rod at a distance of a few centimeters. Ions which have sufficient angular momentum orbit about the rod in the attractive field and oscillate along its length in the axial well produced by the grounded cylinder ends. In addition, the structure forms a coaxial cavity resonant in the TE_{011} mode near $\Delta\nu_2$ with a Q of about 1000.

The 304Å photon detectors are CuBe electron multipliers shielded from metastable neutrals (e.g. ^3He 2^1S_0, 2^3S_1) by 800 Å Aluminium foils. The foils have about 55% transmission at 300 Å.

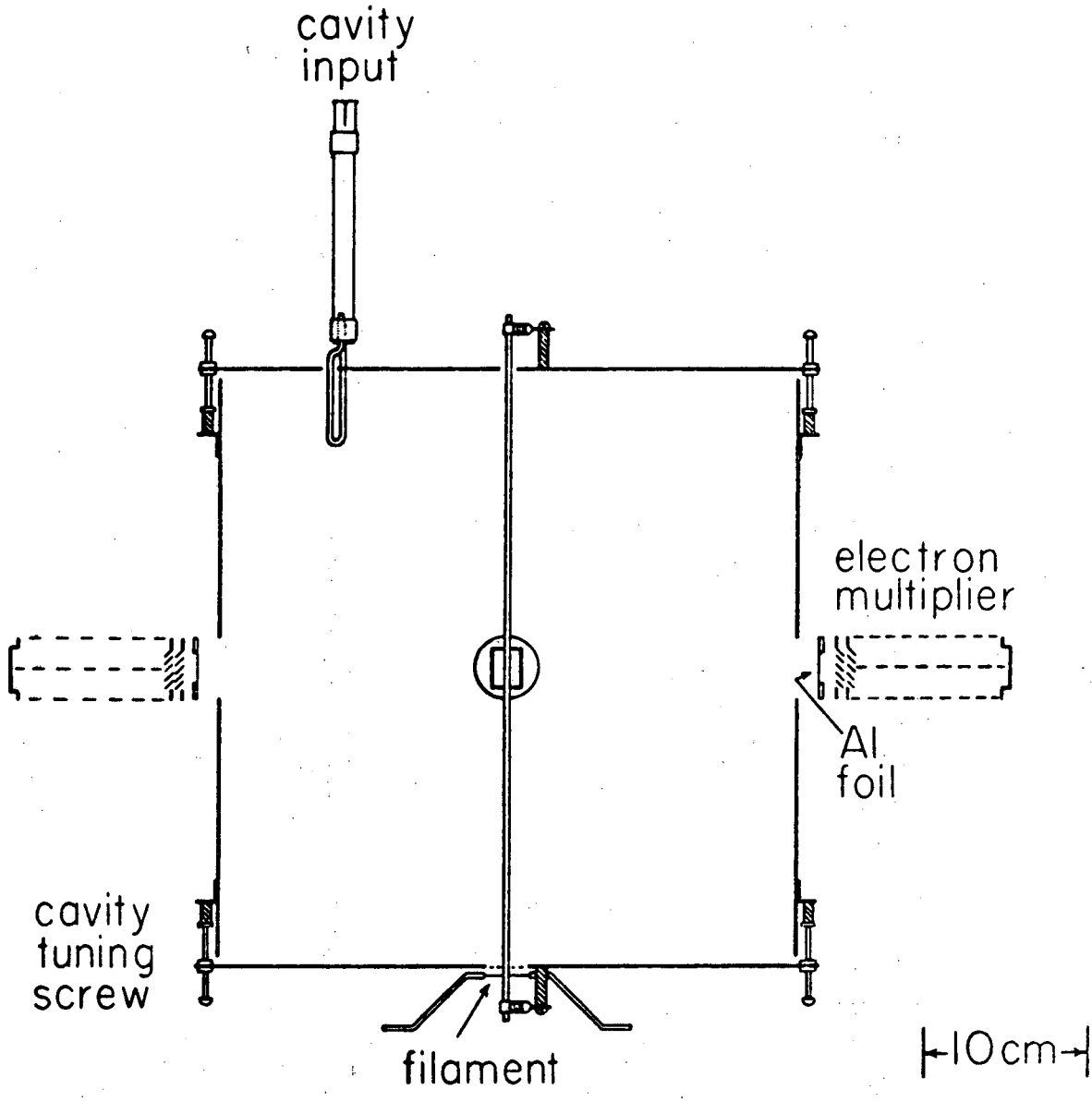

Fig. 2 Sketch of the electrostatic ion trap/rf cavity and photon detectors. The rod is maintained at a negative potential with respect to the closed cylinder during ion confinement. The rectangular shape shown behind the rod center is the microwave horn used to induce 2s to $2p_{\frac{1}{2}}$ transitions.

Fig. 3 shows some of the equipotential surfaces and electric field lines for the static trapping field. They are calculable from the Fourier-Bessel series:

$$\Phi(r,z) = \sum_{n=1,3,5\cdots}^{\infty} [A_n I_o(k_n r) + B_n K_o(k_n r)] \cos k_n z,$$

$$k_n = \pi n / z_{max},$$

$$A_n = -B_n K_o(k_n r_o)/I_o(k_n r_o),$$

$$B_n = (-1)^{\frac{n-1}{2}} \frac{4V_R}{\pi n} \frac{I_o(k_n r_o)}{I_o(k_n r_o)K_o(k_n r_i) - K_o(k_n r_o)I_o(k_n r_i)},$$

with I_o and K_o the zeroth order modified Bessel functions and V_R the potential on the rod.

This type of ion trap has a very simple electrode structure and serves well for the present work where long storage times are not important and the possibility of making the structure a simple rf cavity was advantageous. It is possible, however, to refine the idea of electrostatic ion confinement to allow fairly long confinement times and harmonic motion parallel to the z-axis. In particular consider the cylindrically symmetric potential

$$\Phi'(r,z) = \frac{k}{2}\left(z^2 - \frac{r^2}{2} + B \ln r\right) + C.$$

For B = 0, this potential describes the electric field used in Penning traps and the equipotentials are hyperbolas of revolution about the z-axis. The $\ln r$ term is the potential of a long charged wire and $\Phi'(r,z)$ is a solution of Laplace's equation for arbitrary B. The effective potential U(r,z) acting on an ion of charge q, mass m and having angular momentum L about the z-axis is then,

$$U(r,z) = q\Phi'(r,z) + \frac{L^2}{2mr^2}$$

or,

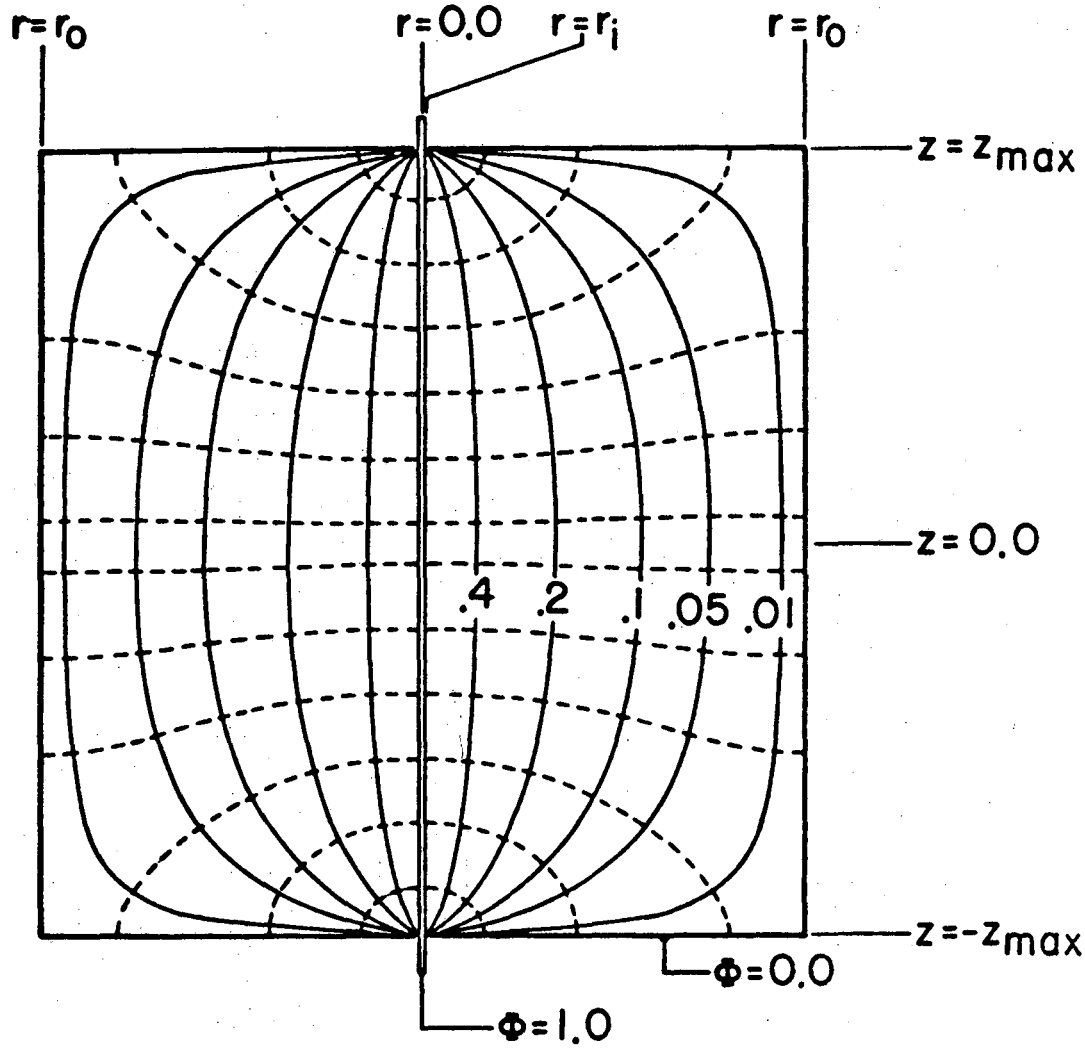

Fig. 3 Potential and field lines for the cylindrical electrostatic ion trap.

$$U(r,z) = \psi(r) + \tfrac{1}{2}kqz^2 + C ,$$

where

$$\psi(r) = q\frac{k}{2}(B\ell nr - \frac{r^2}{2}) + \frac{L^2}{2mr^2} .$$

Thus for $0 < L^2 < (B^2mq/8)$ and qk, $B > 0$ there exist potential wells in the r and z directions which allow ion confinement. Furthermore, the z_1 component of ion motion will be harmonic with frequency $\omega_z = (qk/m)^{\frac{1}{2}}$.

The author and R. Knight have constructed and partially tested a trap whose surfaces conform to equipotentials of $\phi'(r,z)$; it has confined N_2^+ ions for several seconds at pressures of a few times 10^{-9} torr and shows promise of longer confinement times at lower pressures.

DATA COLLECTION AND MEASUREMENT PROCEDURE

The data collection scheme and apparatus is shown in Fig. 4. In analogy to atomic beam nomenclature (A, C and B-magnets) we denote the three sequential time intervals as t_A, t_C and t_B. Counts received from the detectors during the B period are stored in a multi-channel scalar (MCS) whose channel address controls the frequency of a synthesizer from which the power to drive the hyperfine transition is derived. Repetitive scans of the resonance are made with about 1000 data cycles at each MCS address during each scan.

The resonance curves were expected and found to fit the Rabi form

$$S(\nu) = AL(\nu)\sin^2[\pi t_c bL(\nu)^{-\frac{1}{2}}] + C ,$$

with

$$L(\nu) = b^2/[b^2 + (\nu - f)^2] ,$$

where f is the line center, A and C are amplitude and base line parameters and b is the magnetic dipole transition matrix element.

Figure (5) shows a series of resonance curves taken at varying values of t_c. The curves are least squares computer fits to the

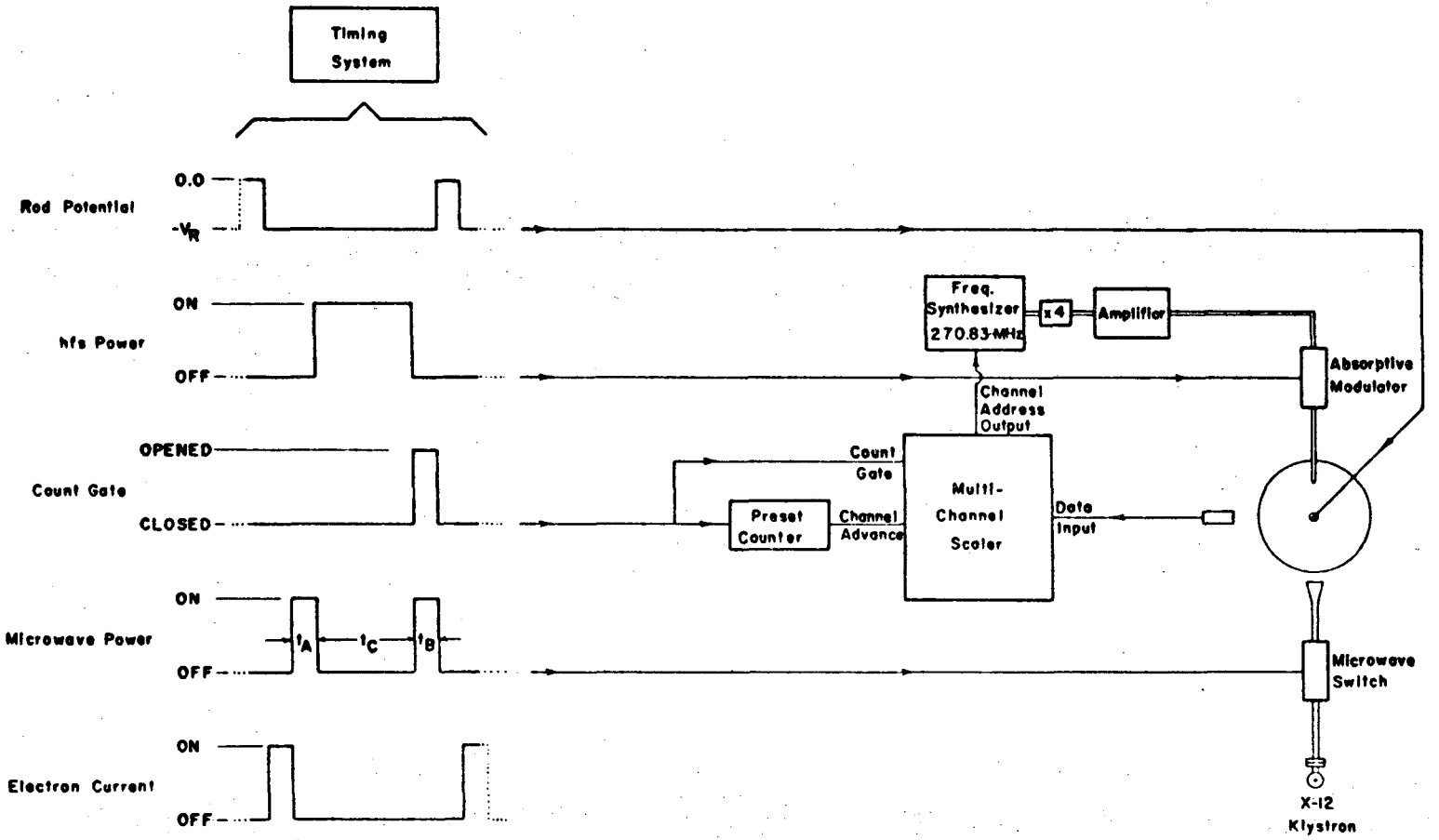

Fig. 4 Sketch of the timing and data collection scheme.

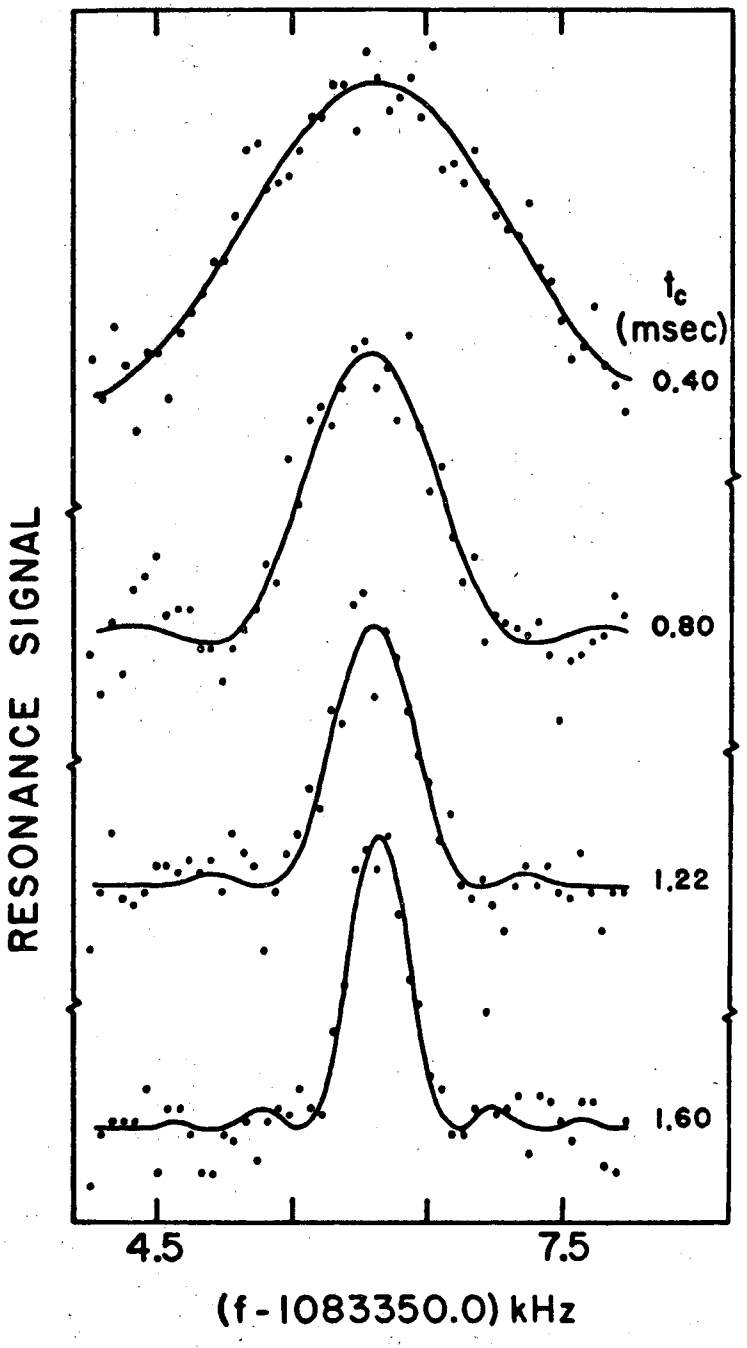

Fig. 5 Resonance curves taken with differing values of t_c. The solid lines are computer fits to the data. The resonance amplitude is typically 20% of the baseline.

data using the Rabi line shape and, though the side bumps don't show here, other data taken at higher values of rf field show them quite plainly.

The $\Delta F = 1$, $\Delta m_F = 0$ transition has a weak quadratic magnetic field dependence given by

$$f(\text{MHz}) = \Delta\nu_2 + (3.615 \times 10^{-3})H^2$$

where H is in gauss. We use three sets of orthogonal Helmholtz coils to allow arbitrary adjustment of the net field about zero. In fact, we use the observed line centers plotted versus magnet coil current to establish the minimum resonant frequency which we take as our primary measurement of $\Delta\nu_2$. Various corrections to values obtained this way are then applied to achieve a final value for $\Delta\nu_2$.

Fig. 6 shows an example of the measurement procedure. Each resonance curve required about one hour to accumulate and thus one determination of the minimum frequency (nominal zero field hfs) took about six hours. Our new result is based on 36 such determinations.

To eliminate the Stark effect on the hfs, we accumulated data at three rod potentials and extrapolated the mean values of the results to zero rod potential. Fig. 7 shows this procedure.

RESULTS AND DISCUSSION

Table II contains a summary of our data and the various corrections applied to achieve our final result:

$$\Delta\nu_2 = 1083.354\ 982\ 5(76)\ \text{MHz}$$

Taken with the $\Delta\nu_1$ value of Scheussler et al.[8],

$$\Delta\nu_1 = 8665.649\ 867(10)\ \text{MHz},$$

we obtain,

$$D_{21} = 1.189993(62)\ \text{MHz}$$

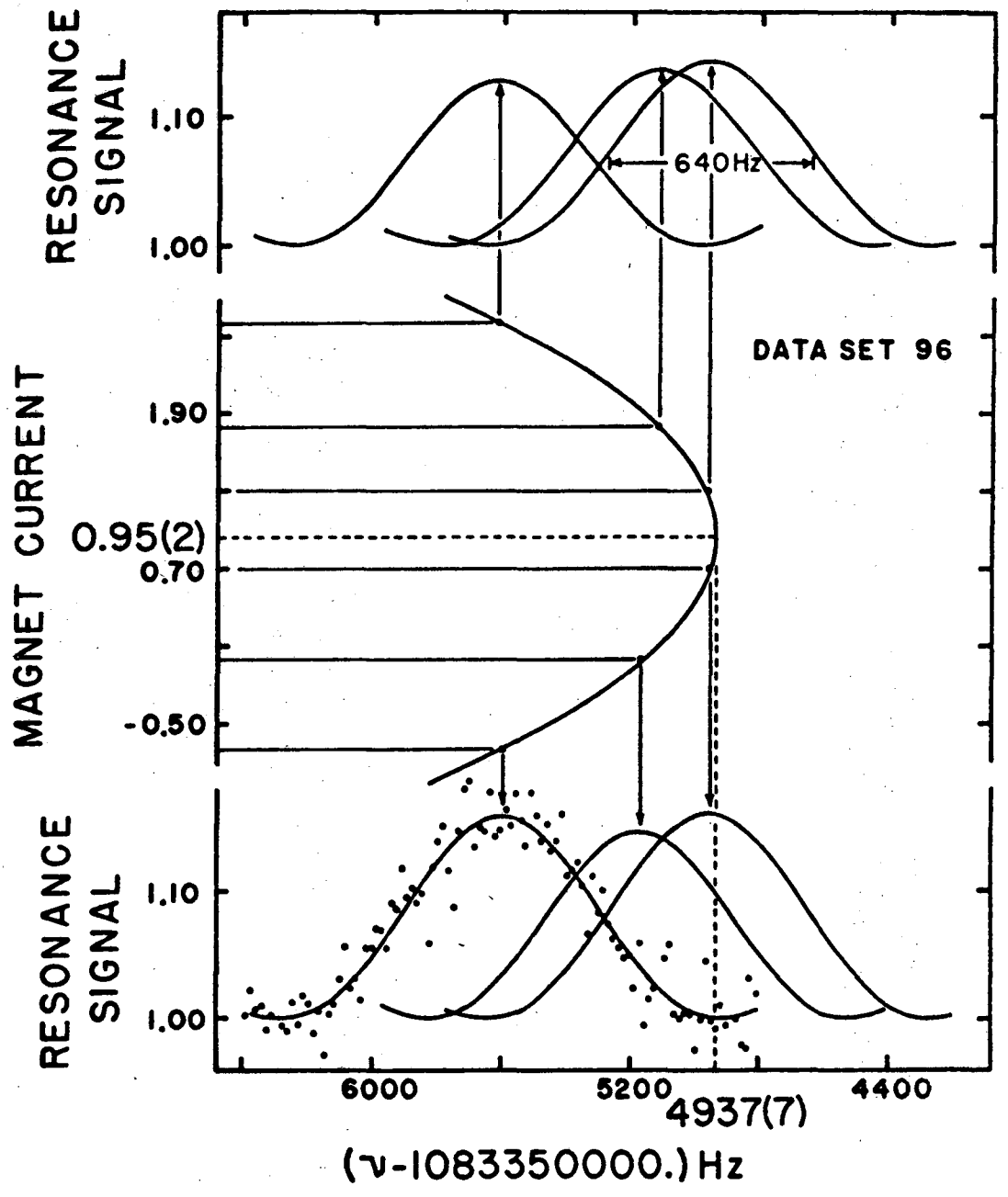

Fig. 6 Variation of resonance line center with Helmholtz magnet current. The solid curves are computer fits. The minimum frequency is the uncorrected hyperfine frequency. Our result is based on 36 such determinations.

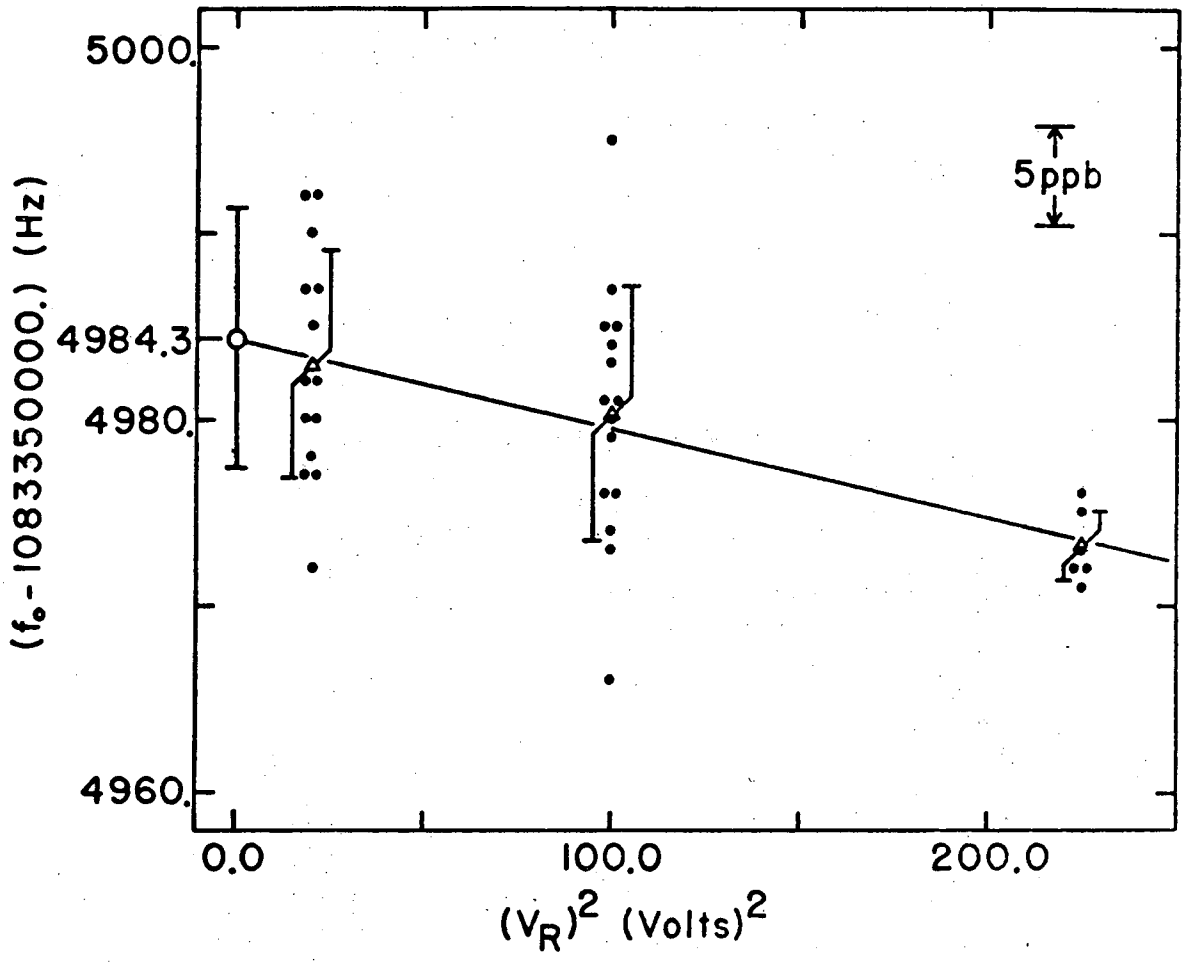

Fig. 7 Extrapolation of zero magnetic field line centers to zero rod potential. The triangles are mean values with 1σ error bars.

The theoretical expression for D_{21} is,

$$D_{21} = E_F \cdot (b_{21} + q_{21} + \delta_{21})$$

where $b_{21} = b_2 - b_1$, $q_{21} = q_2 - q_1$ and $\delta_{21} = \delta_2 - \delta_1$ are the differences in the Breit, QED and nuclear corrections for the 2s and 1s states. δ_2 and δ_1 include nuclear size, polarizability and recoil corrections. E_F is the 1s non-relativistic Fermi contact hfs for a point nucleus,

Table II Summary of Data, Corrections and Result

mean values	V_R = -15.0 V	1083 354 973.2(19) Hz
of zero field	V_R = -10.0 V	980.3(69)
line centers.	V_R = -4.5 V	982.9(61)
$V_R^2 = 0$ Extrapolated Value		1083 354 984.3(70)

Corrections (to be added to $V_R^2 = 0$ value):

a) motional averaging of inhomogeneous magnetic field	-3.2(17)
b) offset of rms averaged residual field from minimum value	-1.3(13)
c) rf Stark effect	0.2(1)
d) 2nd order Doppler shift	0.5(4)
e) pressure shift	2.0(20)

Net result: $\Delta\nu_2$ = 1083 354 982.5(76)Hz

$$E_F = \frac{8}{3}Z^3\alpha^2 R_\infty c g_I \frac{m}{M_p}(I + \tfrac{1}{2}) \left[\frac{M}{M+m}\right]^3$$

where E_F is in frequency units and m, M_p and M are the electron, proton and nuclear masses; the other quantities have their usual meanings. The Breit contribution is,

$$b_{21} = \frac{5}{8}(Z\alpha)^2 + \frac{179}{128}(Z\alpha)^4 + \mathcal{O}(Z\alpha)^6$$

The QED terms calculated to date are[19,20],

$$q_{21} = \frac{\alpha}{\pi}(Z\alpha)^2[-3.30320\ln(Z\alpha) - 5.5515].$$

The recoil terms through order $(Z\alpha)^2$ m/M and second order hfs which contribute to δ_{21} have been calculated by Sternheim[23]. δ_{21} may be partitioned as $\delta_{21} = r_{21} + s_{21}$ where r_{21} are the terms calculated by Sternheim and s_{21} is everything remaining, principally the uncalculated nuclear size contribution.

For $^3He^+$ one obtains;

$$b_{21}E_F = 1.152978(1)(MHz),$$

$$q_{21}E_F = 0.036026(MHz),$$

$$r_{21}E_F = 0.000797(MHz),$$

For a net value of

$$D_{21}\ (theory) = 1.189801(1)(MHz).$$

The difference D_{21} (exp) - D_{21} (theory) = 192 (62) Hz appears to be significant. It is anticipated that the next uncalculated term in q_{21} will make a contribution of order $\alpha(Z\alpha)^3 \cdot E_F = 197$Hz. It is also probable that s_{21} will begin to contribute at this level. Sessler and Foley[22] have calculated s_1 values of -180 and -143 ppm depending on the nuclear wave function used, this would mean that a $s_{21} = -1.5\times10^{-4} \cdot s_1$ would account for the difference in the theoretical and experimental values of D_{21}. In addition, P. Mohr[24] has indicated that for a reasonable nuclear model, $s_{21} \cdot E_F$ in $^3He^+$ is of about the same absolute size as the observed difference in the D_{21} values. It probably will require an evaluation of both s_{21} and the higher order q_{21} term to establish an explanation of the difference between current theory and experiment for D_{21} in $^3He^+$.

ACKNOWLEDGEMENT

Many valuable discussions with Dr. Peter J. Mohr have occurred and we acknowledge them gratefully.

REFERENCES

*Work supported by the Energy Research and Development Administration.

1. G.H. Dunn in Atomic Physics 4, G. zu Putlitz, E.W. Weber, and A. Winnacher, Editors, Plenum Press, New York and London, (1975), p. 575; see also F.L. Walls and G.H. Dunn, Physics Today, 27, 30 (1974).

2. H.G. Dehmelt in Atomic Physics, B. Bederson, V.W. Cohen and F.M.J. Pichanick, Editors, Plenum Press, New York (1969) p. 475.

3. R. Ifflander and G. Werth, Fifth International Conference on Atomic Physics (Abstracts), R. Marrus, M.H. Prior and H.A. Shugart, Editors; Berkeley, Calif. (1976), p. 404.

4. R. Van Dyck, Jr., P. Ekstrom, and H. Dehmelt, Bull. Am. Phys. Soc. 21, 818 (1976); Fifth International Conference on Atomic Physics (Abstracts), R. Marrus, M.H. Prior and H.A. Shugart, Editors; Berkeley, Calif. (1976), p. 336.

5. M.H. Prior, H.A. Shugart, Phys. Rev. Lett. 27, 902 (1971); M.H. Prior, Phys. Rev. Lett. 29, 611 (1972).

6. C. Barnett, et al., in the 1974 Review of the Research Program of the Division of Controlled Thermonuclear Research, ERDA-39, (1975) p. 143.

7. M.H. Prior and E.C. Wang, Phys. Rev. Lett. 35, 29 (1975)

8. H.G. Dehmelt Advances in Atomic and Molecular Physics Vol. 3, Academic Press, New York (1967) p. 53; Vol. 5, (1969) p. 109.

9. H.A. Schuessler, E.N. Fortson and H.G. Dehmelt, Phys. Rev. 187, 5 (1969).

10. F.G. Major and G. Werth, Phys. Rev. Lett. 30, 1155 (1973).

11. H.G. Dehmelt and F.G. Major, Phys. Rev. Lett 8, 213 (1962); H.G. Dehmelt and K.B. Jefferts, Phys. Rev. 125, 1318 (1962).

12. K.H. Kingdon, Phys. Rev. 21, 408 (1923).

13. W.G. Mourad, T. Pauly and R.G. Herb, Rev. Sci. Instr. 35, 661 (1964)

14. R. Novick and E.D. Commins, Phys. Rev. 111, 822 (1958).

15. K.B. Jefferts, Phys. Rev. Lett: 20, 39 (1968); 23, 1476 (1969).

16. H.W. Hellwig, Proc. IEEE 63, 212 (1975).

17. H. Hellwig, et al., IEEE Trans. Instr. Meas. IM-19, 200 (1970).

18. B.E. Lautrup, A. Peterman and E. de Rafael, Phys. Reports 3, 193 (1972) .

19. D.E. Zwanziger, Phys. Rev. 121, 1128 (1961).

20. P.J. Mohr, private communication, has provided an improved value for a numerical integration in Ref. 19.

21. S.J. Brodsky and G.W. Erickson, Phys. Rev. 148, 26 (1966).

22. A.M. Sessler and H.M. Foley, Phys. Rev. 98, 6 (1955).

23. M.M. Sternheim, Phys. Rev. 130, 211 (1963).

24. P.J. Mohr, Private Communication.

TECHNICAL INFORMATION DIVISION
LAWRENCE BERKELEY LABORATORY
UNIVERSITY OF CALIFORNIA
BERKELEY, CALIFORNIA 94720